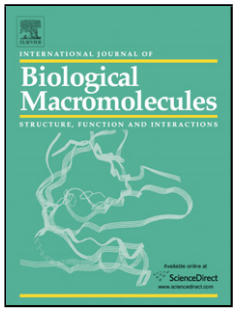

Title: Specific and highly efficient condensation of GC and IC DNA by polyaza pyridinophane derivatives

Authors: Marijana Radić Stojković, Jorge Gonzalez-Garcia, Filip Šupljika, Cristina Galiana-Rosello, Lluis Guijarro, Salvatore A. Gazze, Lewis W. Francis, Ivo Piantanida, Enrique Garcia-Espana

PII: S0141-8130(17)34319-2
DOI: https://doi.org/10.1016/j.ijbiomac.2017.11.156
Reference: BIOMAC 8636

To appear in: *International Journal of Biological Macromolecules*

Received date: 2-11-2017
Revised date: 24-11-2017
Accepted date: 25-11-2017

Please cite this article as: Marijana Radić Stojković, Jorge Gonzalez-Garcia, Filip Šupljika, Cristina Galiana-Rosello, Lluis Guijarro, Salvatore A.Gazze, Lewis W.Francis, Ivo Piantanida, Enrique Garcia-Espana, Specific and highly efficient condensation of GC and IC DNA by polyaza pyridinophane derivatives, International Journal of Biological Macromolecules https://doi.org/10.1016/j.ijbiomac.2017.11.156

Specific and highly efficient condensation of GC and IC DNA by polyaza pyridinophane derivatives

Marijana Radić Stojković[†,b], Jorge Gonzalez-Garcia[†,a], Filip Šupljika[d], Cristina Galiana-Rosello[a], Lluis Guijarro[a], Salvatore A. Gazze[c], Lewis W. Francis[c], Ivo Piantanida[*,b], Enrique Garcia-Espana[*,a]

[a]Department of Inorganic Chemistry, Institute for Molecular Science, University of Valencia, Catedratico Jose Beltran 2, 46980 Paterna (Spain)

[b]Division of Organic Chemistry & Biochemistry, Ruđer Bošković Institute, P. O. Box 180, 10002 Zagreb (Croatia)

[c]Institute of Life Science II, Swansea University Medical School, (UK).

[d]Faculty of Food Technology and Biotechnology, University of Zagreb, Pierrotijeva 6, 10002 Zagreb (Croatia)

[*]Corresponding Authors: Enrique Garcia-Espana (enrique.garcia-es@uv.es), Ivo Piantanida (Ivo.Piantanida@irb.hr)

[†]Marijana Radić Stojković and Jorge Gonzalez-Garcia contributed equally.

Graphical abstract

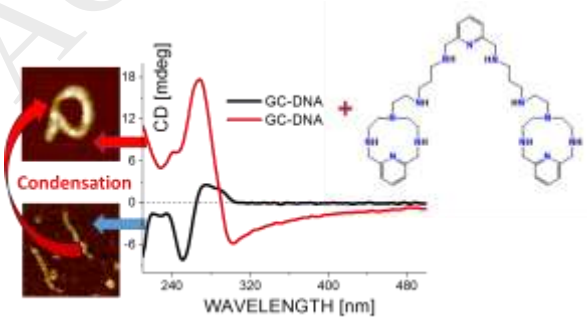

Abstract

Two bis-polyaza pyridinophane derivatives and their monomeric reference compounds revealed strong interactions with ds-DNA and RNA. The bis-derivatives show a specific condensation of GC- and IC-DNA, which is almost two orders of magnitude more efficient than the well-known condensation agent spermine. The type of condensed DNA was identified as ψ-DNA, characterized by the exceptionally strong CD signals. At variance to the almost silent AT(U) polynucleotides, these strong CD signals allow the determination of GC-condensates at nanomolar nucleobase concentrations. Detailed thermodynamic characterisation by ITC reveals significant differences between the DNA binding of the bis-derivative compounds (enthalpy driven) and that of spermine and of their monomeric counterparts (entropy driven). Atomic force microscopy confirmed GC-DNA compaction by the bis-derivatives and the formation of toroid- and rod-like structures responsible for the ψ-type pattern in the CD spectra.

List of abbreviations

AFM → Atomic Force Microscopy

AT-DNA → poly dA – poly dT

CD → circular dichroism

ctDNA → *calf thymus* DNA

ds-DNA → double stranded DNA

$\Delta_r G^o$ → Gibbs free energy

$\Delta_r H^o$ → enthalpy

$\Delta_r S^o$ → entropy

EB → ethidium bromide

EMF → electromotive force

ESI → electronic supplementary information

GC-DNA → poly $(dGdC)_2$ or poly dG – poly dC

IC-DNA → poly $(dIdC)_2$

ICD → induced CD spectrum

ITC → Isothermal titration calorimetry

K_a → equilibrium association constant

LD → linear dichroism

N → [bound ligand] / [polynucleotide]

ψ-DNA → psi-DNA (condensed form)

poly dAdT → poly dA – poly dT

poly AU → poly A – poly U

S → spermine

T_m → melting temperature

Keywords

pyridinophane compounds • DNA/RNA binding • GC-DNA condensation •circular dichroism spectroscopy

Introduction

Naturally occurring polyamines, such as spermine, spermidine and putrescine are ubiquitous cellular cations that play key roles in cell growth, differentiation[1], cell progression and apoptosis.[2,3] Growth regulation by polyamines is partly associated with their nucleic acids interaction and ability to alter DNA conformation through condensation and aggregation.[4,5] Stabilization of specific DNA conformations is important for processes such as nucleosome formation,[6] chromatin condensation[7] and gene expression.[8,9] Moreover, a high polyamine

concentration is linked with the initiation and progression of cancer.[10] Therefore, the study of the interactions of novel polyamine-like compounds with DNA and RNA polynucleotides is still of great relevance in biomedical chemistry. The main stabilizing driving force between polyamines and nucleic acids is an electrostatic interaction between the positively charged polyamines and the negatively charged phosphates of nucleic acids. Moreover, the ability of polyamines to change their protonation degree upon small pH variations permits to modulate the interaction with DNA. However, interactions with the bases along the grooves should also be taken into account. For example, spermine is reported to have either weak or no base-pair selectivity[11,12] or GC selectivity[13,14] depending on the base-composition of the DNA duplexes. On the other hand, natural polyamines induce changes from the B-secondary DNA structure to the A- or Z- structures[Error! Bookmark not defined.] and can favour DNA aggregation processes.[Error! Bookmark not defined.] In this frame, our groups launched a program to develop synthetic open-chain polyamine ligands able to bind selectively RNA over DNA[15] However, the first family of ligands exhibited negligible *in vitro* activity in cancer cell cultures due to a poor cellular uptake caused by their high charge at physiological conditions. In order to improve cell uptake, we prepared aryl-linked (pyridine and phenanthroline) bis-polyaza pyridinophane ligands (**L2** and **L5** in Scheme 1) with the same charge as the previous family but possessing a much higher hydrophobicity due to their bulky conformation induced by an internal hydrogen bond network[16] The selectivity achieved by these polyazapyridinophane ligands for ds-RNA (poly A–poly U) over ds-DNA (poly dA–poly dT) was explained by the differences in the steric properties of the binding sites of these polynucleotides.[17] Interestingly, the much lower ds-RNA over ds-DNA selectivity observed for **L5** in comparison to **L2** was ascribed to the ability of phenanthroline to intercalate between the base-pairs of the polynucleotides.

The pronounced ds-RNA over ds-DNA selectivity showed by **L2** is intriguing and has led us to perform a more detailed study of the interaction of **L2**-like compounds with DNA and RNA.

Following this approach, we have synthesized a new poly pyridinophane ligand **L1** (Scheme 1) with a higher number of amino groups than **L2** but retaining the same conformation and preserving some of the properties of the parent aryl linked compounds **L2** and **L5**. In addition, we have studied ligands **L3** and **L4** (Scheme 1) described as the one-arm monomer counterparts of **L1** with and without the pyridine unit in the arm, respectively.

We have studied the interaction of these ligands with double stranded polynucleotides presenting significant differences in the secondary structure: i) ctDNA which presents a classical B-helix and mixed base pair composition[18], ii) dGdC-DNAs which also form classical B-helix but with a minor groove that is sterically hindered by amino groups of guanine, iii) the close analogue dIdC-DNA lacking the amino groups in the purine bases, iv) dAdT-DNA which forms a peculiar twisted secondary structure characterized by much narrower and deeper minor groove[19] in comparison to common B-helix of other ds-DNAs and v) rArU-RNA (ds-RNA) characterized by A-helical structure of wide and shallow minor groove and deep and narrow major groove.**Error! Bookmark not defined.**

Taking into account the preliminary circular dichroism experiments of the interaction of **L2** and poly dG-poly dC which suggested DNA condensation, we have expanded our studies to all bis- and mono-derivative compounds shown in Scheme 1 by using thermal UV melting, CD and ITC techniques. In addition, an acyclic polyamine that is a well-known DNA condensation agent in cells, spermine, was studied for comparative aims. **Error! Bookmark not defined.**[20]

Results and discussion

Synthesis and acid-base behaviour

*Synthesis of the compounds **L1-L4**.*

The synthesis of **L1** was carried out by reacting two moles of 6-(6-amino-3-azahexyl)-3,6,9-triaza-1-(2,6)-pyridinecyclodecaphane (**L4** in Scheme 1) with one mole of pyridine-2,6-

dicarboxaldehide in dry ethanol followed by *in situ* reduction with sodium borohydride. Finally, **L1** was precipitated as its hydrochloride salt with HCl in dioxane. Synthesis of **L2**, **L3** and **L4** was achieved as previously reported.[Error! Bookmark not defined.,21] All the ligands were characterized by NMR spectroscopy, HR-MS and elemental analysis (see Material and Methods)**.**

*Acid-base behaviour of **L1-L4**.*

Potentiometric titrations were conducted to know which species prevail in solution and to determine the number of charges of the ligands in the pH range of interest. The protonation constants of **L1** along with those of **L2, L3** and **L4,** reported previously, are shown in Table S1.[Error! Bookmark not defined.,Error! Bookmark not defined.,22] **L1** presents eight protonation steps in the pH range of study (pH = 2.5 – 10.5) and the high values of the protonation constants make the species $H_8\mathbf{L1}^{8+}$ to prevail in a wide pH range (see figure S1 in ESI). From the analysis of the distribution diagrams (figures S1-S2), the net charges of the ligands at pH 7.0 were calculated and shown in Table 1. The net charges follow the trend **L1** > **L2** > **L4** ~ **L3** (Table 1), which is in good agreement with the increasing number of secondary amine groups in the ligands.

Interactions of L1-L4 compounds with double stranded nucleic acids

Thermal denaturation studies

It is well known that when heated, ds-helices of polynucleotides dissociate into two single stranded polynucleotides at well-defined temperatures (T_m value). The thermal stability of ds-polynucleotides, and thus the T_m value, is affected by the binding of non-covalent small molecule. In this regard, T_m differences between free polynucleotides and their complexes with small molecules (ΔT_m values), are an important factor in the characterisation of small molecule / ds-polynucleotide interactions.[23] Thermal denaturation studies of compounds **L1-L4** and spermine with ds-DNA (ctDNA, poly dAdT, poly $(dIdC)_2$) and ds-RNA (poly AU) were performed and ΔT_m values are collected in Table 2.

L1-L4 did not exhibit significant stabilization effect in the studied polynucleotides except for poly A – poly U. On the other hand, spermine, the simplest polyamine of the series, exhibited the largest ds-polynucleotide stabilization. This effect is possibly related to its acyclic- structure that allows for a more efficient interaction between its ammonium groups and the phosphate backbone groups.[24]

Both, bis-derivatives (**L1**-**L2**) and mono-derivatives (**L3**-**L4**), demonstrated stronger stabilization of ds-RNA (poly A-poly U) than of ds-DNA (poly dA – poly dT).**Error! Bookmark not defined.** Taking into account the conformations of these polynucleotides, the observed thermal denaturation selectivity is probably related to the much deeper major groove of ds-RNA that allows a more efficient binding of all polyamine-based compounds.

Specific trends in the stabilization effects of poly dA – poly dT (ΔT_m values) and ratios (***r*** = [Ligand)] / [polynucleotide]) were observed for both single- and double-derivatives. **L3** (***r*** =0.5, ΔT_m = 3.3) and **L4** (***r*** =0.5, ΔT_m = 3.9) showed an increase of poly dA – poly dT stabilization with the increase of ***r*** whilst **L1** showed an opposite trend (decrease in stabilization with the increase of ***r***). The stabilization pattern of single-derivatives is of typical minor groove binders (namely higher stabilization with an increase of ***r***).[25] The opposite effect observed for **L1** (ΔT_m (***r*** = 0.1) = 5.9 > ΔT_m (***r*** = 0.2) = 3.5 > ΔT_m (***r*** = 0.5) = 2.4) suggests that this bulkier double-derivative cannot bind as properly in the minor groove of poly dA – poly dT as it does for low molar ratios. This effect may be induced by modification of AT minor groove dimensions that hampers the binding of additional molecules.[26]

A small stabilization of the mixed base-pair composition, ctDNA (42% of GC base-pairs and 58 % of AT base-pairs) was only shown by spermine. Furthermore, low ΔT_m values were observed for poly $(dIdC)_2$ with **L1**, **L2** and spermine.

ITC titrations of compounds with ds-DNA and ds-RNA

Isothermal titration calorimetry (ITC) is the only experimental technique that allows the calculation of all components of the Gibbs' equation simultaneously in a single experiment at a given temperature (the binding constant equilibrium (K_a), Gibbs free energy of binding ($\Delta_r G^o$), enthalpy ($\Delta_r H^o$), entropy ($\Delta_r S^o$) and the stoichiometry (N) of the association event (see Experimental Section and ESI for details).[27,28,29]

The majority of titration experiments resulted in negative peaks indicating that the binding processes were exothermic (Figure 1 and ESI). The most of the resulting data was fitted to a single-site binding model by using a nonlinear least square method (Table 3).

Analysis of ITC experiments of the double-derivatives **L1** and **L2** and of the single-derivative **L3** with poly dA – poly dT, poly A – poly U and poly dG – poly dC showed relatively high and similar binding affinities (log K_a in Table 3) with the binding stoichiometries ranging from 0.11 to 0.21. A correlation between the binding thermodynamic parameters, the number of ligand net charges and the chemical structural features (one *vs.* two polyazamacrocyles and propylamine-chain extension) was observed following the series **L1** > **L2** > **L3**. An exception occurs for the interaction of the compounds with poly dA – poly dT which presents similar $\Delta_r G^o$ and K_a values. Aside from the ligand structure, the type of polynucleotide plays an important role in the binding process and hence, in the thermodynamic parameters. Therefore, $\Delta_r H^o$ and $T\Delta_r S^o$ values increase following the polynucleotide trend: poly dA – poly dT (the non-classical B helix conformation**Error! Bookmark not defined.** with the slow solvent exchange rates in the minor groove[30,31]) > poly dG – poly dC (an intermediate A/B-helix) > poly A – poly U (A-helix).

A strikingly different thermodynamic signature was observed for the single derivative **L3** compared to the double-derivatives **L1** and **L2**. The interaction of **L3** with poly A – poly U and poly dG – poly dC was characterized by positive (favourable) binding entropies ($T\Delta S^o$ term) and slightly negative enthalpies (Table 3), revealing an entropically driven binding. On the other hand, the binding of both bis-derivative ligands (**L1** and **L2**) with polynucleotides was

favoured by the large negative enthalpy and the significant negative entropy terms, indicating overwhelmingly enthalpically driven binding processes. In many cases, the groove binding is associated with positive (favourable) binding entropies due to the release of confined or interfacial water molecules to the bulk as we postulated for **L3** from the thermal studies.[Error! Bookmark not defined.,32]

The enthalpic contribution to the free energy reflects the specificity and the strength of interactions occurring between the binding partners (ionic and hydrogen bonds, electrostatic and van der Waals interactions, polarisation of the interacting groups and others).[Error! Bookmark not defined.] On the other hand, the stronger interaction in a bimolecular binding process will produce a more negative enthalpy that occurs at the expense of an increased order, leading to a more negative entropy contribution (see Tables 3 and 4).

In order to analyse the differences in ITC profiles of alternating dGdC and dIdC sequences, spermine and double-derivative compounds were also titrated with poly $(dGdC)_2$ and poly $(dIdC)_2$. Poly $(dGdC)_2$, titrations with both **L1** and **L2** exhibited binding constants of an order of magnitude higher than of the other polynucleotides. Experiments of double-derivatives with poly $(dIdC)_2$ were processed according to a two sites model, since both **L1** and **L2** demonstrated two types of binding (Figure 1, S7 and S12 in ESI).

The first binding event with dIdC sequences was characterized by binding constants of two orders of magnitude higher than those for the other polynucleotides studied.

Unlike spermine, where binding was clearly entropy driven, the titrations with **L1** and **L2** was accompanied by almost equally large negative ΔH^o values and positive $T\Delta S^o$ terms. All thermodynamic parameters obtained from spermine titrations with dGdC and dIdC sequences are in agreement with previous reports.[Error! Bookmark not defined.,33]

Lower constants and small negative entropies were obtained for the second type of binding of both double-derivatives with poly $(dIdC)_2$.

Ethidium bromide displacement assays

As an alternative method for the estimation of affinity of small molecules for polynucleotides, we have performed ethidium bromide (EB) displacement assays (ESI, Figures S37 - S38). It should be stressed that this method gives only an estimation of the affinity, since the difference in binding modes (intercalation of EB *vs* groove binding of compounds) and the difference in the molecule size between EB and **L1, L2** does not allow a direct comparison of binding affinity.

Taking into account the obtained IC_{50} values (ESI, Table S2) and the binding constant of EB toward ctDNA in the same experimental conditions (pH 7.0, log Ks = 6), the estimated affinity of **L1, L2** toward ds-polynucleotides is about log *Ks* 6, and for **L3** log *Ks* 5, which agrees within an order of magnitude with the ITC results (Table 3).

CD spectroscopy

CD spectroscopy, a highly sensitive method for detecting conformational changes in the secondary structure, was used to monitor changes in polynucleotide properties induced by small molecule binding.[34] In addition, achiral small molecules such as **L1**-**L3** can eventually acquire induced CD spectrum (ICD) upon binding to polynucleotides, potentially providing useful information of the binding modes .[35,36] However, the absorbance range of DNA and **L1**-**L3** strongly overlaps, thus only changes in CD spectra at $\lambda > 290$ nm could be attributed to eventual ICD bands of small molecules.

In general, the addition of the single-derivative **L3** to polynucleotides caused negligible changes in CD spectra (see Figures S29-S33 in ESI) and thus will not be further discussed.

The appearance of a negative CD band in the 295 - 300 nm region, was observed as a common feature of all CD titrations with **L1** and **L2** (Figures 2 and 3 and S29-S33 in ESI). While the

addition of **L1**-**L2** to ds-polynucleotides yielded only very small changes in CD spectra at r < 0.2. (see Figure 2), at higher ratio (r > 0.2, Figure 2) changes in CD spectra became significant. The addition of **L1** and **L2** to poly dA - poly dT and poly A - poly U yielded similar effects coupled with the rise of a negative ICD band above 295 nm and exclusively in poly dA - poly dT titrations, a concomitant hypsochromic shift of polynucleotide CD maximum (Figure S31 in ESI).

Most intriguingly, the addition of **L1** and **L2** to GC-based polynucleotides resulted in the dramatic changes of CD spectra (Figures 2 and S30 in ESI), characterized by a strong intensity increase of CD-bands and strong shifts of CD maxima. Such exceptional changes led us to perform a detailed CD study of the double-derivatives with various GC-DNAs; poly dG-poly dC, poly $(dGdC)_2$ and its close analogue poly $(dIdC)_2$ (Figures 2, S30, S32-S33 in ESI). For comparison, the well-known GC-DNA condensing agent spermine (**S**) was also studied in our experimental conditions.**Error! Bookmark not defined.**.**Error! Bookmark not defined.**

Poly dG – poly dC adopts an unusual B-form with some distinctly A-like features.[37] Even though embedded G-tracts have a propensity to favour the A-form in solution**Error! Bookmark not defined.**, the overall conformation of (G+C) rich DNA fragments was more indicative of the B-form.[38] First additions of both **L1** and **L2** ($r_{[L]/[polynucleotide]}$ = 0.1) caused transition of poly dG – poly dC to the A-form with a characteristic negative peak at 210 nm (Figure S30 in ESI). Unusually for the A-form, another peak appeared at 270 nm, likely due to the cumulative effect of ICD bands of **L1** and **L2** combined with changes in CD spectrum of DNA. Further additions (r > 0.2) resulted in dramatic intensity increases of the CD bands, which can be attributed to the condensation of poly dG – poly dC (see Figure 2). It is noteworthy that condensation occurred at lower ratio for **L1** (r = 0.3) than for **L2** (r = 0.5), which could be explained by the higher charge of **L1** at this pH (**L1**, +6; **L2**, +4.2, see Table 1). Similarly to the bis-derivatives (**L1**-**L2**), the addition of the mono-derivative **L3** to a poly dG – poly dC solution also resulted in a

transition to the A-form but contrary to **L1** and **L2**, the condensation did not happen which emphasizes the importance of the second polyaza chain.

Even stronger changes in CD spectrum were observed at lower ratios ($\boldsymbol{r} \leq 0.1$) for the alternate GC-base polynucleotide (poly $(dGdC)_2$), suggesting a higher propensity of the compounds to condense this particular DNA (see Figure 2 middle and S32 in ESI). Nonetheless, the strongest increase in CD bands was observed for poly $(dIdC)_2$ (Figure 2 up and S33 in ESI). Poly $(dIdC)_2$ is a peculiar DNA that lacks the purine 2-amino group and exhibits a rather unusual CD spectrum[39] having a positive peak near 264 nm and a negative band at 284 nm characteristic of a Z-DNA structure. Nevertheless, vacuum CD[40,41], Raman[42] and NMR[43] studies indicate that poly $(dIdC)_2$ forms the right-handed B-DNA double helix.

The strong changes in CD spectra of GC and IC polynucleotides induced by the double-derivatives are characterized by (i) a negative signal around 300 nm, (ii) the large magnitude CD bands compared to the intrinsic CD bands of studied polynucleotides and (iii) an extension of CD bands to the non-absorbing region in the form of CD tails. All these features in CD spectra could be attributed to the formation of ψ (psi) form-DNA induced by **L1**-**L2**.

The ψ -DNA[44,45] is considered to be a twisted and tightly packaged self-assembly of the polymer, which is postulated to occur when 90% of the DNA negative charge from the phosphate backbone is neutralized.[46]

The transition from the B-DNA to the ψ-DNA is reversible and could be monitored by CD spectroscopy by changing the ionic strength of the solution ($I \geq 0.1$M). Therefore, the initial CD spectra of the **L2**-poly $(dGdC)_2$ complex in the ψ-DNA form showed the expected ψ → B transition upon NaCl addition (Figure 3). Moreover, the flow-LD experiments of the **L1**-ctDNA complex were performed and they confirmed DNA condensation by the appearance of an intense LD band induced by **L1** addition (Figure S36 in ESI). **Error! Bookmark not defined.**,[47]

Spermine (**S**) was studied by CD spectroscopy as the well-known DNA-condensing reference agent.[Error! Bookmark not defined.,Error! Bookmark not defined.] Although **S** induced a B → A transition in poly dG – poly dC (see Figure S30 in ESI) similar to **L1-L2**, at high ratios it did not yield any condensation. For alternating dGdC and dIdC DNA, **S** induced profound changes in the CD spectra consistent with the ψ (psi) - DNA profile. However, to observe these changes an order of magnitude higher ratio was required for **S** ($r > 1.1$) than for **L1 - L2** ($r_] \geq 0.1$).

To estimate the impact of GC polymer length on the condensation process, we carried out the CD experiment with alternating GC 25mer and **L1** (Figure S34 in ESI). The positive CD band at 283 nm shifted towards shorter wavelengths at $r = 0.1$, while the large magnitude CD band appeared at $r = 0.2$, pointing to a DNA-condensation similar to that observed for poly $(dGdC)_2$. Interestingly, the negative signal near 300 nm was not present in the CD spectrum of GC 25mer in contrast to poly $(dGdC)_2$. Additionally, the reversible ψ → B transition experiment with **L1**-GC 25 mer complex was successfully obtained upon addition of NaCl (see ESI).

Discussion of calorimetric and spectroscopic studies

The degree of polynucleotide condensation was different depending on the basepair composition and their secondary structure and varied following the trend poly A – poly U < poly dA – poly dT < poly dG – poly dC < poly$(dGdC)_2$ < poly$(dIdC)_2$. Although **L1** and **L2** bind in the major groove of both poly dG – poly dC (the intermediate A/B-DNA) and poly A – poly U (A-RNA), only poly dG – poly dC showed a pronounced condensation (Figure 2, Figure S29 in ESI). These effects can be related to different electrostatic potential around DNA and RNA that brings ions closer to the latter than to the former. Also, the computations of the potential around DNA and RNA duplexes showed that the major groove of A-RNA has a higher negative potential than the minor groove while this is reversed for B-DNA. Because of that, multicharged ions have a tendency to bury themselves very deep within the RNA major groove

and thus, are not visible at the surface.[48,49] On the other hand, in less deep DNA major grooves (i.e. poly dG – poly dC) multivalent cationic substrates can be more accessible from outside and the condensation is likely to occur when the surface charge patterns can electrostatically contact with each other.

Also, our findings that spermine (+4) is capable of inducing the condensation of alternating GC sequences (Figure S32 in ESI) and not of consecutive GC sequences (Figure S30 in ESI), suggested that the intrinsic DNA structure is an additional important factor in inducing the condensation beside the basepair composition. As mentioned earlier, although both poly dG – poly dC and poly $(dGdC)_2$ belong to the B-form of DNA, consecutive GC tracts can adopt structures between B-form and A-form in solution and depending on the local water activity, can be more prone to B $\rightarrow$ A transition.[50]

Although the binding to nucleic acids and DNA condensation represent complex processes, we propose possible simplified explanations for the obtained thermodynamic profiles of studied ligand-polynucleotide systems (Tables 3 and 4):

1) a first type of binding occurring in the minor groove of AT and IC sequences and in the major groove of GC and AU sequences was accompanied by removal of the sequence-dependent hydration patterns from the binding site (entropy-driven) and forming the specific interactions (hydrogen bond interactions, van der Waals attractions, hydrophobic forces) inside the binding site (mostly enthalpy-driven), 2) the second type of binding occurring after the saturation of dominant binding sites was probably accompanied by a partial displacement of bound molecules from the binding site followed by partial recovery of water molecules from bulk solution to the binding site and electrostatic interactions of ligand molecules with the backbone phosphates. Thus, the noticed decrease in stabilization of poly dA – poly dT upon the increase of **L1** concentration could result from the partial displacement of **L1** molecules from the minor groove (Table 2). Whether this second type of binding will be characterized by the larger

favourable enthalpy or the larger favourable entropy contribution to the Gibss free energy, depends on lots of factors (the size and the number of net positive charges of the ligand, differences in structure-dependent and sequence-dependent hydration of polynucleotides[51], differences in electrostatic potentials around DNA/RNA and inside the binding sites[52], the shape of minor and major groove, the specificity of ligand-polynucleotide interaction). It appears from the thermodynamic profile of spermine-GC/IC systems that the favourable entropic contribution is mostly the result of the electrostatic binding rather than specific interactions inside the binding site. Interestingly, despite the similar negative electrostatic potentials in the minor grooves of AT and IC sequences, stabilization of poly dA – poly dT was higher compared to that of poly $(dIdC)_2$ (Table 2). The reason for this can be a narrower minor groove of poly dA – poly dT that enables the deep penetration of ligands and the better interaction conditions inside the minor groove. Another reason for the lower stabilization of poly $(dIdC)_2$ could be the binding of ligands not only inside the minor groove but also inside the major groove due to the equally negative electrostatic potentials in those binding sites.**Error! Bookmark not defined.** The possibility of favourable binding to two binding sites could enable ligands with higher number of net positive charges to better screen charges at poly $(dIdC)_2$ backbone and thus to induce stronger condensation of that polynucleotide. Obtained experimental results (strong condensation of poly $(dIdC)_2$ in contrast to weak condensation of poly dA – poly dT) support that assumption. Further, a better condensation of alternating GC sequences could result from less negative electrostatic potential in the major groove compared to that of GC homopolymer.**Error! Bookmark not defined.**

Agarose gel electrophoresis

Extensive agarose gel electrophoresis is commonly used for investigating the DNA cleavage efficiency and the various binding modes of small molecules to supercoiled DNA.[53] Gel

electrophoresis can also be used to monitor the effect of DNA condensation induced by different ligands.[54] We performed this assay (Figure 4) to evaluate the impact of **L1 - L3** and spermine binding to DNA (plasmid BlSc r2.9) and, consequently, to investigate the relative mobility of the formed complexes at different compound/DNA concentration ratios. Bis-polyaza pyridinophane compounds (**L1** and **L2)** strongly delayed the mobility of DNA at 50 μM concentration, while at ten times lower concentration (5 μM) there was no effect. Spermine decreased the mobility of DNA only at 50-times higher concentration (5 mM) while monomer ligand, **L3** had no effect on DNA mobility. These results agree with the tendency to condense DNA observed in the CD experiments; **L1** and **L2** have a stronger ability to condense DNA than spermine while **L3** has no effect on DNA condensation.

Atomic Force Microscopy

Atomic Force Microscopy (AFM) is a surface-sensitive technique able to describe 3D conformations of biomolecules at high nanometer level resolution. In this work, AFM was employed to visualise poly $(dGdC)_2$ conformation deposited on atomically flat mica surface, before and after the addition of condensing agents (Figure 5). Figure 5A shows DNA molecules on a mica surface, with the expected elongated conformation of a linear ds-DNA polymer. The addition of **L1** at $\boldsymbol{r}$ = 0.3 resulted in the condensation of the polynucleotide, with the increase in height, width (Table 5) and the acquisition of a rod-like and toroid-like morphology (Figure 5B-C). Compaction effects on poly $(dGdC)_2$ was also caused by the well-known condensing polyamine agent spermine at $\boldsymbol{r}$ = 1.2 (Figure 5D). The observed conformational changes in topography are in line with the formation of supercoiled DNA in condensing environments, where the presence of positive charges screens the negatively-charged DNA backbone and induces DNA compaction[55,56,57]. The same environment can generate different topographies, such as rods, toroids and spheroids[Error! Bookmark not defined.], which may as well represent different

stages of the condensation process[Error! Bookmark not defined.]. The high increase in dimensions with **L1** (Figure 5B-C) is caused by the formation of multi-molecular condensed polynucleotide, as reported previously for other condensing agents[58]. This can be ascribed to the more efficient condensing effect of **L1** compared to spermine, which could drive the aggregation of a larger number of poly $(dGdC)_2$ molecules. AFM measurements reported here give visual and structural complementary information of the condensation of poly $(dGdC)_2$ as observed with the CD spectroscopy in the present study.

Conclusions and Outlook

Our study confirms that electrostatic and hydration forces are the main driving forces in ligand-induced condensation processes of DNA/RNA by highly positively charged ligands. In contrast to the published literature, the interaction of polyaza double-derivatives **L1** - **L2** with DNA/RNA is enthalpy driven, whereas DNA/RNA interactions of similarly positively-charged spermine and the single polyaza derivative **L3** are entropy driven. This difference stresses the importance of the ligand supramolecular organisation upon the target binding, whereby only **L1** and **L2** possess the so called 'tweezer' structural features that provide the ability to wrap around DNA/RNA binding sites.

Furthermore, we have shown that the DNA/RNA condensation capacity is closely related to the binding site properties (shape and electrostatic potential) as well as to the features of the multivalent ligands (**L1**, **L2** charge, structure and size). The condensation was negligible in poly A – poly U and poly dA – poly dT but strongly pronounced in GC- and IC-DNAs. Upon binding to poly dG – poly dC, all four studied compounds (**L1**, **L2**, **L3** and spermine) at low ratio, $\boldsymbol{r}$ = 0.1, converted B-DNA to A-DNA, but only the bis-derivatives **L1** and **L2** showed additional structural and charge capacity to induce transition from A-DNA to a condensed, ψ-DNA form.

Particularly interesting is the specific and exceptionally strong CD response to GC- and IC-DNA condensation induced by **L1** and **L2**. For instance, upon addition of **L1** and **L2**, a 20-50-fold increase of CD-band at 260 nm was observed for the GC/IC-DNA sequences which allowed the determination of nanomolar concentrations of DNA-bases.

In particular, the results presented herein highlight the differences between mono-(**L3**,**L4**) and bis-cyclic (**L1**,**L2**) derivatives. Moreover, there is an evident difference in DNA-condensation efficiency between linear amines (spermine-S, and many other analogues) and the here used cyclic amines. A plausible reason might be that at physiological pH both secondary amine groups of the macrocyclic core are protonated and they can establish hydrogen bonds with unprotonated amino groups of the bridge or with the pyridine connector giving rise to a close conformation in which most of the heteroatoms are oriented inwards providing a restricted hydrophobic environment. Previous modelling studies performed for **L2** and **L5**[Error! Bookmark not defined.] showed that the conformations is dependent on the protonation state acquiring the molecules a much extended or open conformation at acidic pH values when the extensive protonation of the secondary ammonium groups disrupts the hydrogen bonding network. Linear polyamines, being less bulky, can easily fit in the grooves and adjust the original shape of oligonucleotides, in that way less favouring the aggregation.

The results here presented provide means to distinguish between different polynucleotide duplexes using polyaza ligands and give basic information about the thermodynamics of these recognition processes in physiological conditions (~0.15 M NaCl, 37 ^{o}C). Further detailed *in vitro* studies may afford additional insight into the possible biological applications of bis-polyaza pyridinophane derivatives. The planned experiments will be conducted by means of transient transfection of the HeLa cells with pECFP-Mito vector and the commercial transfecting agent Lipofectamine 2000 as a control. In addition, many protein coding genes consist of GC-rich isochores,[59] also certain regions of the human genome, including the

regulatory regions of oncogenes, and the Epstein Barr virus genome, have very high guanine-cytosine contents (>80%)[60]. Thus, selective GC-DNA condensing ligands[61,62]can be relevant for the control of gene expression and thereby, for the treatment of genetic diseases, infections by antibiotic-resistant bacteria or cancer.

Experimental Section

Synthesis of L1. 2,6-Pyridinedicarboxaldehyde (0.3 g, 2.0 mmol) were dissolved in 40.0 mL of anhydrous ethanol and added dropwise to **L3** (1.0 g, 4.2 mmol) dissolved in 30.0 ml of anhydrous ethanol during 1 hours. The mixture was stirred additionally for 2 hours and $NaBH_4$ (0.9 g, 20.7 mmol) was then added and the resulting solution stirred for 2 hours at room temperature. Therefore, the ethanol was removed under reduced pressure, extracted with H_2O (30.0 mL) and CH_2Cl_2 (3 x 25.0 mL) and dried over $MgSO_4$. The organic phase was removed at reduced pressure, and the resulting residue was dissolved in ethanol and precipitated as hydrochloride salt of **L1** in 63% yield. mp: 223–225 ^oC. ^1H NMR (300.0 MHz, D_2O): δ (ppm) = 7.64 (t, 2H, *J* = 8 Hz), 7.63 (t, 1H, *J* = 8 Hz), 7.18 (d, 2H, *J* = 8Hz), 7.13 (d, 4H, *J* = 8Hz), 4.32 (s, 8H), 4.18 (s, 4H), 3.11-3.16 (m, 4H), 2.85-2.96 (m, 12H), 2.62-2.65 (m, 8H). ^{13}C NMR (75.4 MHz, D_2O): δ (ppm) = 140.1, 139.7, 123.5, 122.5, 51.4, 51.2, 50.9, 49.8, 46.3, 43.5. Calc for $C_{33}H_{51}N_{11}\cdot 6HCl\ 4H_2O$: C, 44.4; H, 7.3; N, 17.3. Found: C, 44.6; H, 7.7; N, 16.5. *MS* (*FAB*) *m*/*z* 601.0 $[M]^+$

EMF measurements. The potentiometric titrations were carried out at 298.1 ± 0.1 K using NaCl 0.15 M as supporting electrolyte. The experimental procedure (burette, potentiometer, cell, stirrer, microcomputer *etc.*) has been fully described elsewhere.[63] The acquisition of the EMF data was performed with the computer program PASAT.[64] The reference electrode was an Ag/AgCl electrode in saturated KCl solution. The glass electrode was calibrated as a hydrogen ion concentration probe by titration of previously standardized amounts of HCl with

CO_2-free NaOH solutions and the equivalent point determined by the Gran's method,[65] which gives the standard potential, $E^{0'}$,and the ionic product of water (pK_w = 13.7(1)). The computer program HYPERQUAD was used to calculate the protonation and stability constants.[66] The HYSS[67] program was used to obtain the distribution diagrams The pH range investigated was 2.5-11.0.

Study of DNA/RNA interactions. The UV/Vis spectra were recorded on a Varian Cary 100 Bio spectrophotometer, CD spectra were recorded on JASCO J815 spectropolarimeter at 25.0 ^oC using appropriate 1 cm path quartz cuvettes. For study of interactions with DNA and RNA, aqueous solutions of compounds buffered to pH = 7.0 (Na cacodylate buffer, I = 0.05 mol dm^{-3}). Polynucleotides were purchased as noted: poly dGdC – poly dGdC, poly dIdC – poly dIdC, poly dAdT – poly dAdT, poly dG – poly dC, poly dA – poly dT, poly A – poly U, (Sigma), calf thymus ctDNA (Aldrich). Polynucleotides were dissolved in sodium cacodylate buffer, I = 0.05 mol dm^{-3}, pH = 7.0. The calf thymus ctDNA was additionally sonicated and filtered through a 0.45 μm filter.[68] Polynucleotide concentration was determined spectroscopically as the concentration of phosphates[69]. CD experiments were performed by adding portions of compound stock solution into the solution of polynucleotide on a JASCO J815 spectrophotometer.

Thermal melting curves for ds-DNA, ds-RNA and their complexes with studied compounds were determined as previously described[Error! Bookmark not defined.] by following the absorption change at 260 nm as a function of temperature. Absorbance of the ligands was subtracted from every curve and the absorbance scale was normalized. T_m values are the midpoints of the transition curves determined from the maximum of the first derivative and checked graphically by the tangent method.[Error! Bookmark not defined.] The ΔT_m values were calculated subtracting T_m of the free nucleic acid from T_m of the complex. Every ΔT_m value here reported was the average of at least two measurements. The error in ΔT_m is ± 0.5 °C.

ITC measurements. ITC experiments were performed by means of an isothermal titration microcalorimeter Microcal VP-ITC (MicroCal, Inc. Northampton, MA, USA) at 25.0°C. Origin 7.0 software, supplied by the manufacturer, was used for data acquisition and treatment. In the titration experiments, aliquots of the ligand (see ESI for detailed protocol) were injected from a rotating syringe (307 rpm) into the calorimeter reaction cell containing polynucleotide solution (ESI). Blank experiments were carried out to determine the heats of dilution of the ligands and the polynucleotides. All solutions used in the ITC experiments were degassed under vacuum prior to use to eliminate air bubbles. Each injection generated a heat burst curve (P in μW versus time). The data were imported to Origin 7.0 and the area under each peak was determined by integration to evaluate the heat associated with the injection. The data were corrected for heats of dilution. The resulting data were analysed by using the Origin 7.0 software according to the model based on a single set or two set of identical binding sites to estimate the binding contants (K_a), the binding stoichiometry (N) and the enthalpy of binding ($\Delta_r H^o$). The reaction Gibbs energies ($\Delta_r G^o$) were calculated by using the following equation: $\Delta_r G^o = -RT\ln(K_a)$.

Entropic contribution to the binding Gibbs energy was calculated by equation: $T\Delta_r S^o = \Delta_r H^o - \Delta_r G^o$.

Ethidium bromide (EB) displacement assay[70]**:** to polynucleotide solution ($c = 9.0 \times 10^{-6}$ mol dm^{-3}) ethidium bromide was added ($\boldsymbol{r}_{[\mathbf{EB}]/\ [\text{polynucleotide}]}$=0.3), and quenching of the **EB**/polynucleotide complex fluorescence emission (λ_{ex}=520 nm, λ_{em}=602 nm) was monitored as function of c(**EB**)/c(compound). The given IC_{50} values present the ratio c(**EB**)/c(compound) = [Int(**EB**/polynucleotide) – Int($\mathbf{EB}_{free}$)] / 2, where Int(**EB**/polynucleotide) is fluorescence intensity of **EB**/polynucleotide complex and Int($\mathbf{EB}_{free}$) is fluorescence intensity of the free ethidium bromide before polynucleotide is added.

Agarose gel electrophoresis. The gel electrophoresis was performed on a 1.5% agarose in TAE buffer (pH = 8.0), using TAE as a running buffer[71], applying constant voltage of 50.0 V for one hour, followed by quick staining of the gel with EB solution (0.5 μg/mL).

Atomic Force Microscopy*:* An Atomic Force Microscope Bruker BioScope Catalyst (Bruker Instruments, Santa Barbara, California, USA) was used to visualize DNA deposited on freshly-cleaved mica flakes. The measurements were performed in 40 mM HEPES buffer (pH 7.4) with $NiCl_2$ (1 mM). Samples consisted of 7.6×10^{-7} M poly $(dGdC)_2$ alone or in combination with spermine or compound **L1.** The ratio condensation agent/polynucleotide,***r*** was 0.12 and 0.30 for spermine and **L1**, respectively. The samples were incubated on mica flakes for 10 min at room temperature, then imaged in the same buffer or rinsed with MilliQ water and dried under a gentle stream of nitrogen. For analysis in air, RTESP cantilevers (Bruker Instruments, Santa Barbara, California, USA) were used, with a nominal spring constant of 40 N/m and a nominal resonant frequency of 300.0 kHz. For imaging in buffer, MLCT-E cantilevers were used (Bruker Instruments, Santa Barbara, California, USA), with a nominal spring constant of 0.05 N/m and a nominal resonant frequency of 26.0 kHz. All imaging was conducted using Tapping Mode and Peak Force Tapping Mode at a scan speed of 1Hz. Images were processed with first-order flattening and dimensions of molecules were calculated using Bruker Nanoscope Analysis software and ImageJ software.

Author Contributions

The manuscript was written through contributions of all authors. All authors have given approval to the final version of the manuscript.

Acknowledgements

Financial supports from Croatian Science Foundation (grant No. 1477), from Ministry of Science, education and sports (Project No.098-0982914-2918), FP7-REGPOT-2012-2013-1, Grant Agreement Number 316289 – InnoMol are gratefully acknowledged.

This work was financially supported by the Spanish MINECO, FEDER funds of the E. U. (Project CTQ2013-14892 and CONSOLIDER INGENIO 2010-CSD2010-00065), Generalitat Valenciana (PROMETEO II 2015-002) and Unidad de Excelencia MDM 2015-0538.

References

[1] A. C. Childs, D. J. Mehta, E. W. Gerner, Cell. Mol. Life Sci. 60 (2003) 1394–1406; S. S. Cohen, A Guide to Polyamines, Oxford University Press, New York, NY, 1998.

[2] T. Thomas, T. J. Thomas, Cell Mol. Life Sci. 58 (2001), 244–258.

[3] K. Igarashi, K. Kashiwagi, Biochem. Biophys. Res. Commun. 271 (2000) 559–564.

[4] L. C. Gosule, J. A. Schellman, J. Mol. Biol. 121 (1978) 311-326.

[5] M.-H. Hou, S.-B. Lin, J.-M. P. Yuann, W.-C. Lin, A. H.-J. Wang, L. Kann, Nucleic Acids Res. 29(24) (2001) 5121–5128.

[6] M. M. Garner, G. Felsenfeld, J. Mol. Biol. 196 (1987) 581–590; B. G. Feuerstein, N. Pattabiraman, L. J. Marton, Nucleic Acids Res. 18(5) (1990) 1271–1282.

[7] D. Sen, D. M. Crothers, Biochemistry 25 (1986) 1495-1503; I. V. Smirnov, S. I. Dimitrov, V. L. Makarov, J. Biomol. Struct. Dyn.5 (1988) 1149–1161.

[8] Y. Huang, L. J. Marton, P. M. Woster, R. A. Casero, Essays Biochem. 46 (2009) 95–110.

[9] A. Rich, A. Nordheim and A.H.-J. Wang, Ann. Rev. Biochem. 53 (1984) 791–846.

[10] U. Bachrach, Basic Mechanisms and Clinial Approaches, in: K. Nishioka (Eds.), Polyamines in Cancer, Landes Bioscience Publishers, Austin, TX, 1996, pp. 45-74.

[11] S. Hirschman, M. Leng, G. Felsenfield, Biopolymers 5 (1967) 227–233; J. E. Morgan, J. W. Blankenship, H. R. Matthews, Arch. Biochem. Biophys. 246 (1986) 225–232.

[12] M. M.Patel, T. J. Anchordoquy, Biophys. Chem. 122 (2006) 5–15.

[13] M. Yuki, V. Grukhin, C.-S. Lee, I.S. Haworth, Arch. Biochem. Biophys. 325 (1996) 39–46.

[14] H. Deng, V. A. Bloomfield, J. M. Benevides, G. J. Thomas, Nucleic Acids Res. 28 (2000) 3379–3385; R. Marquet, A. Wyart and C. Houssier, Biochim. Biophys. Acta 909 (1987) 165–172.

[15] A. Sornosa-Ten, M. T. Albelda, J. C. Frías, E. García-España, J. M. Llinares and A. Budimir, I. Piantanida, Org. Biomol. Chem. 8 (2010) 2567–2574.

[16] J. Gonzalez, J. M. Llinares, R. Belda, J. Pitarch, C. Soriano, R. Tejero, B. Verdejo and E. García-España, Org. Biomol. Chem. 8 (2010) 2367–2376.

[17] J. González-García, L. Uzelac, M. Kralj, J. M. Llinares and E. García-España, I. Piantanida, Org. Biomol. Chem. 11 (2013) 2154–2161.

[18] C. R. Cantor, P. R. Schimmel, Biophysical Chemistry, WH Freeman and Co., San Francisco, 1980, p.1109.; W. Saenger, Principles of nucleic acid structure, Springer-Verlag, New York, 1984, p 220

[19] W. D. Wilson, Y.-H. Wang, C. R. Krishnamoorthy, J. C. Smith, Biochemistry 24 (1985) 3991–3999.

[20] V. A. Bloomfield, Biopolymers 44 (1997) 269–282.

[21] M. Inclan, M. T. Albelda, J. C. Frías, S. Blasco, B. Verdejo, C. Serena, C. Salat-Canela, M. L. Díaz, A. García-España, E. García-España, J. Am. Chem. Soc.134 (2012) 9644-9656.

[22] C. Marín, M. Inclán, I. Ramírez-Macias, M. T. Albelda, R. Cañas, M. P. Clares, J. González-García, M. J. Rosales, K. Urbanova., E. García-España, M. Sánchez-Moreno, RSC Adv. 6 (2016) 17446-17455.

[23] J.-L. Mergny, L. Lacroix, Oligonucleotides 13 (2004) 515-537.

[24] H. Ohishi, N. Terasoma, I. Nakanishi, G. van der Marel, J. H. Van Boom, A. Rich, A. H.-J. Wang, T. Hakoshima, K. Tomita, FEBS Lett. 398 (1996) 291-296.

[25] A. Y. Chen, C. Yu, B. Gatto, L.F. Liu, Proc. Natl. Acad. Sci. U. S. A. 90 (1993) 8131-8135.

[26] I. Rouzina, V. A. Bloomfield, Biophys. J. 74 (1998) 3152; T. H. Duong, K. Zakrzewska, J. Biomol. Struct. Dyn. 14 (1997) 691-701.

[27] J. B. Chaires, Arch. Biochem. Biophys. 453 (2006) 26-31.

[28] A. K. Bronowska, Thermodynamics of Ligand-Protein Interactions: Implications for Molecular Design, in: J. C. Moreno PirajÃ¡n (Ed.), Thermodynamics - Interaction Studies - Solids, Liquids and Gases, InTech, 2011, pp.1-48.

[29] R. Perozzo,; G. Folkers and L. Scapozza, J. Recept. Signal Transduct. Res. 24 (2004) 1-52.

[30] V. A. Buckin, B. I. Kankiya, N. V. Bulichov, A. V. Lebedev, I. Ya. Gukovsky, V. P. Chuprina, A. P. Sarvazyan, A. R. Williams, Nature 340 (1989) 321-322; X. Shui, L. McFail-Isom, G. G. Hu, L. D.Williams, Biochemistry 37 (1998) 8341-8355.

[31] Y.Z. Chen, E. W. Prohofsky, Biophys. J. 64 (1993) 1385–1393.

[32] L. A. Marky, K. J. Breslauer, Proc. Natl. Acad. Sci. U. S. A. 84 (1987) 4359-4363.

[33] D. Matulis, I. Rouzina and V. A. Bloomfield, J. Mol. Biol. 296 (2000) 1053-1063.

[34] A. Rodger, B. Norden, Circular Dichroism and Linear Dichroism, Oxford University Press, New York, 1997.

[35] N. C. Garbett, P. A. Ragazzon, J. B. Chaires, Nat.Protoc. 2 (2007) 3166-3172.

[36] M. Eriksson, B. Nordén, Linear and Circular Dichroism of Drug-Nucleic Acid Complexes, in: J. B. Chaires, M. J. Warin (Eds.), Methods in Enzymology, Academic Press, San Diego, 2001, 340, pp. 68-98.

[37] L. Trantirek, R. Stefl, M. Vorlickova, J. Koca, V. Sklenar, J. Kypr, J. Mol. Biol. 297 (2000) 907-922.

[38] M. Lindqvist, A. Gräslund, J. Mol. Biol. 314 (2001) 423-432.

[39] M. Vorlícková, J. Sági, Nucleic Acids Res.19 (1991) 2343-2347.

[40] J. C. Sutherland, K. P. Griffin, Biopolymers 22 (1983) 1445-1448.

[41] L. Wang, T. A. Keiderling, Nucleic Acids Res. 21 (1993) 4127-4132.

[42] G. Fabriciová, P. Miškovský, D. Jancura, E. Kočlsová, V. Lisý, Gen. Physiol. Biophys. 14 (1995) 203-216.

[43] P. A. Mirau, D. R.Kearns, Biochemistry 23 (1984) 5439-5446.

[44] Y. A. Shin, G. L. Eichhorn, Biopolymers 23 (1984) 325-335.

[45] T. J.Thomas, R. P.Messner, Nucleic Acids Res. 14 (1986) 6721-6233; T. J . Thomas, T. Thomas, Nucleic Acids Res. 17 (1989) 3795-3810.

[46] R. W. Wilson, V. A. Bloomfield, Biochemistry 18 (1979) 2192-2916.

[47] R. Marrington, T. R. Dafforn, D. J. Halsall, A. Rodger, Biophys. J. 87 (2004) 2002-2012.

[48] K. Chin, K. A. Sharp, B. Honig, A. M. Pyle, Nat.Struct.Mol.Biol. 6 (1999) 1055-1061.

[49] I. S. Tolokh, S. A. Pabit, A. M. Katz, Y. Chen, A. Drozdetski, N. Baker, L. Pollack, A. V. Onufriev, Nucleic Acids Res. 42 (2014) 10823-10831; A. Noy, A. Perez, F. Lankas, F. Javier Luque, M. Orozco, J. Mol. Biol. 343 (2004) 627-638.

[50] H. L .Ng, R. E. Dickerson, Nucleic Acids Res.30 (2002) 4061; S. Arnott, Polynucleotide secondary structures: an historical perspective, in: S. Neidle (Ed.), Oxford Handbook of Nucleic Acid Structure, Oxford University Press, 1999, pp. 1-38.

[51] T. V. Chalikian, J. Völker, A. R. Srinivasan, W. K. Olson, K. J. Breslauer, Biopolymers 50 (1999) 459-471.

[52] R. Lavery, B. Pullman, Nucleic Acids Res.9 (1981) 7041-7051; P. Weiner et. al., Proc. Nat. Acad. Sci. U.S.A. 79 (1982) 3754-3758.

[53] Y. Li, Z. Yang, Inorg. Chim. Acta 362 (2009) 4823-4831; C .P. Tan, J. Liu, L –M. Chen, S. Shi, L–N. Ji, J. Inorg. Biochem.102 (2008) 1644-1653; Q. Wang, W. Li, F. Gao, S. Li, J. Ni, Z. Zheng, Polyhedron 29 (2010) 539-543; G. Zuber, J. C. Jr. Quada, S .M. Hecht, J. Am. Chem. Soc. 120 (1998) 9368-9369.

[54] C. Ma, V. A. Bloomfield, Biopolymers 35 (1995) 211-216.

[55] O. Y. Limanskaya, A. P. Limanskii, Gen. Physiol. Biophys. 27 (2008) 322-337.

[56] V. Vijayanathan, T. Thomas, T. Antony, A. Shirahata, T. J. Thomas, Nucleic Acids Res. 21 (2004) 127-134.

[57] A. L. Martin, M. C. Davies, B. J. Rackstraw, C.J. Roberts, S. Stolnik, S.J.B. Tendler, P.M. Williams, FEBS Letters (2000) 106-112.

[58] J. C. Sitko, E. M. Mateescu, H. G. Hansma. Biophys. J. 84 (2003) 419-431.

[59] F. Alvarez-Valina , G. Lamollea, G. Bernardi, Gene 300 (2002) 161-168; N. Cohen, T. Dagan, L. Stone, D. Graur, Mol. Biol. Evol.22 (2005) 1260-1272.

[60] M. Lee, C. Walker, Sequence-Selective Binding of DNA by Oligopeptides as a Novel Approach to Drug Design, in: R. M. Ottenbrite (Ed.), Polymeric Drugs and drug Administration, 1994, pp 29-46.

[61] M. J. Araúzo-Bravo, A. Sarai, Nucleic Acids Res. 36 (2008) 376-386.

[62] R. Rohs, S. M. West, A. Sosinsky, P. Liu, R. S. Mann, B. Honig, Nature 461 (2009) 1248-1253; M. Lee, A. L. Rhodes, M. D. Wyatt, S. Forrow, J. A. Hartley, Biochemistry 32 (1993) 4237-4245.

[63] E. García-España, M. J. Ballester, F. Lloret, J. M. Moratal, J. Faus, A. Bianchi, J. Chem. Soc., Dalton Trans. (1988) 101-104.

[64] M. Fontanelli, M. Micheloni, Proceedings of the I Spanish-Italian Congress on Thermodinamics of Metal Complexes, Peñíscola, Castellón, 1990, Program for the automatic control of the microburette and the acquisition of the electromotive force readings.

[65] G. Gran, Analyst 77 (1952) 661-671; F. J. Rossotti, H. Rossotti, J. Chem. Educ.42 (1965) 375.

[66] P. Gans, A. Sabatini, A. Vacca, Talanta 43 (1996) 1739-1753.

[67] P. Gans, Programs to determine the distribution of Species in multiequilibria systems from the stability constants and mass balance equations.

[68] J. B. Chaires, N. Dattagupta, D. M. Crothers, Biochemistry 21 (1982) 3933-3340.

[69] G. Malojčić, I. Piantanida, M. Marinić, M. Žinić, M. Marjanović, M. Kralj, K.Pavelić, H.-J. Schneider, Org. Biomol. Chem.3 (2005) 4373-4381.

[70] D. L. Boger, B. E. Fink, S. R. Brunette, W. C. Tse, M. P. Hedrick, J. Am. Chem. Soc. 123 (2001) 5878-5891.

[71] I. Lubitz, D. Zikich, A. Kotlyar, Biochemistry 49 (2010) 3567-3574.

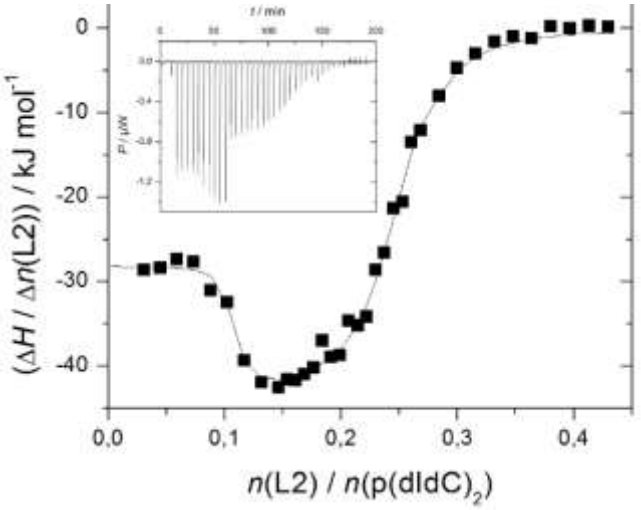

Figure 1. ITC experiments of poly $(dIdC)_2$ titrated with **L2**; experimental data (■) and calculated fit for model *two sets of sites* (—). Insets: raw titration data from the single injection of **L2** into a solution of poly $(dIdC)_2$.

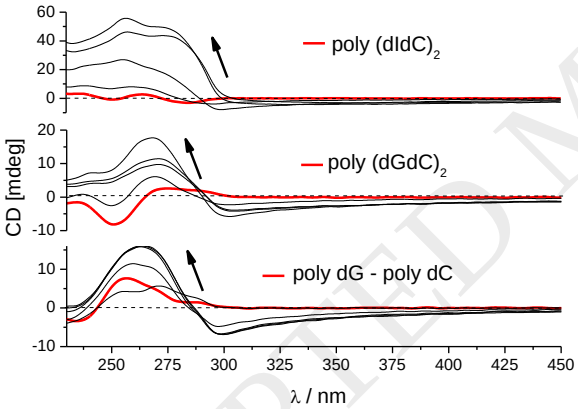

Figure 2. CD titration of poly $(dGdC)_2$, poly $(dIdC)_2$ and poly dG-poly dC ($c = 3 \times 10^{-5}$ M) with **L1** at molar ratios $r_{[\mathbf{L1}]\ /\ [\text{polynucleotide}]} = 0;\ 0.1;\ 0.2;\ 0.3;\ 0.4$ (pH 7.0, buffer sodium cacodylate, $I = 0.05$ M). At $\lambda > 300$ nm (right of vertical dotted line) only **L1** absorbs light and thus positive band in CD could be attributed only to the induced (I)CD band of chromophore.

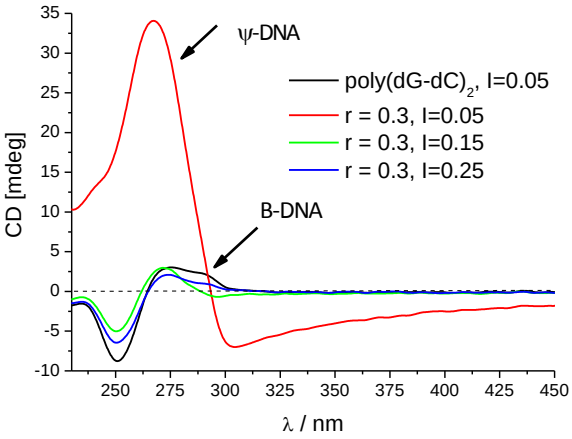

Figure 3. CD spectra of poly (dGdC)$_2$ ($c = 3\times10^{-5}$ M) upon addition of **L2**, at molar ratio $r_{[\mathbf{L2}]\ /\ [\text{polynucleotide}]}$ = 0.3 and subsequent increase of NaCl concentration (pH 7.0, buffer sodium cacodylate, $I = 0.05$ mol dm^{-3}).

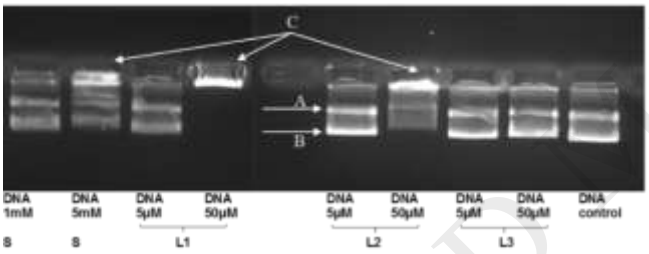

Figure 4. Gel electrophoresis of the supercoiled plasmid DNA, BlSc r2.9. Arrows point A – open circular plasmid DNA, B – supercoiled circular plasmid DNA, C – supercoiled circular plasmid DNA, retained by **L1**, **L2** and spermine; **S**-spermine.

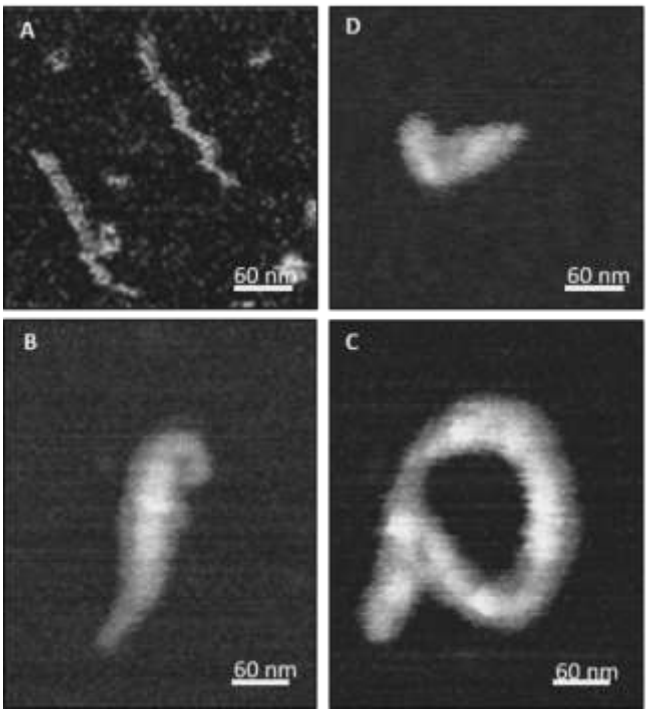

Figure 5. AFM images of poly $(dGdC)_2$ deposited on mica surfaces. (A) Two linear polymers in the absence of condensing agents imaged in buffer (HEPES 40 mM, $NiCl_2$ 1 mM, pH 7.4). Addition of compound **L1** results in the condensation of the poly $(dGdC)_2$ to form rod-like (B) and toroid-like (C) structures. (D) Condensation of the poly $(dGdC)_2$ in the presence of spermine.

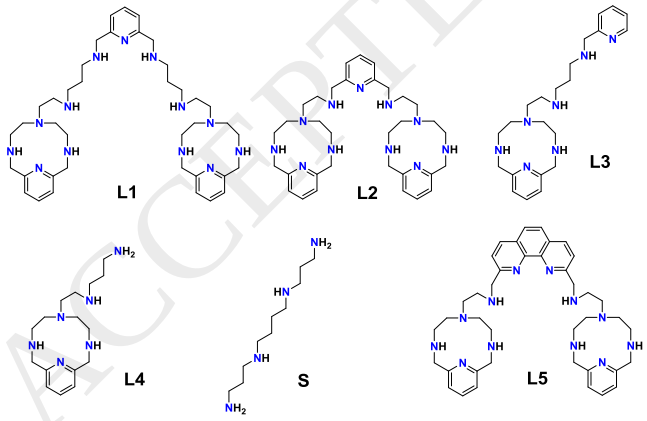

Scheme 1. Structures of **L1 – L4** and spermine (**S**)

Table 1. Number of positive charges resulting from amine protonation for each compound at pH =7.0.[a]

L1	L2	L3	L4
6.0	4.2	3.2	3.4

[a] Calculated by pH-metric titrations in aqueous solution at 298.1 K using 0.15 M NaCl as a supporting electrolyte.

Table 2. ΔT_m[a] values (°C) of studied ds- polynucleotides upon addition of **L1**-**L4** and spermine at pH 7.0 (sodium cacodylate buffer, I = 0.05 M).

	ctDNA		polydAdT		polyAU		poly(dIdC)$_2$
***r*[b]**	0.1	0.2	0.1	0.2	0.1	0.2	0.1
L1	0	0.8	5.9	3.5	27.5	c	1.8
L2	0	-	1.9	c	15.1	c	1.0
L3	0	0	1.0	1.4	1.0	1.5	-
L4	0.5	0.5	0.5	1.6	12.3	15.7	-
S[d]	1.0	2.7	3.4	5.1	23.5	26.1	1.2

[a] Error in $\Delta T_m \pm 0.5$ °C; [b] r = [Ligand] / [polynucleotide]; [c] Precipitation; [d] Spermine

Table 3. Data parameters obtained during nonlinear regression for ITC titration of poly A-poly U, poly dG-poly dC, poly $(dGdC)_2$, poly $(dIdC)_2$ and poly dA-poly dT with compounds **L1**, **L2**, **L3** and spermine with the model *one set of sites.*

		N	log K_a	$\Delta_r H^o$	$T\Delta_r S^o$	$\Delta_r G^o$
				kJ mol^{-1}		
poly A -poly U	**L1**	0.1	7.1	-50.7	-10.4	-40.3
	L2	0.2	6.3	-44.9	-8.6	-36.3
	L3	0.2	6.0	-15.0	19.1	-34.1
poly dG -poly dC	**L1**	0.1	6.9	-60.1	-20.9	-39.2
	L2	0.2	6.3	-51.4	-15.7	-35.7
	L3	0.2	6.0	-13.9	20.3	-34.2
poly dA -poly dT	**L1**	0.1	7.0	-73.8	-33.7	-40.1
	L2	0.2	7.2	-61.2	-20.0	-41.2
	L3	0.2	7.1	-27.3	13.1	-40.4
poly $(dGdC)_2$	**L1**	0.1	8.2	-64.1	-17.1	-47.0
	L2	0.2	8.3	-42.5	4.6	-47.1
	S	2.2	5.0	-0.9	27.5	-28.4
poly $(dIdC)_2$	**S**	2.1	4.5	-2.5	23.0	-25.5

Table 4. Data parameters obtained during nonlinear regression (model: *two sets of sites*) for ITC titration of poly $(dIdC)_2$ with **L1** and **L2**.

	*N*1	log K_a	$\Delta_r H^o$/kJ mol^{-1}	$T\Delta_r S^o$/kJ mol^{-1}	$\Delta_r G^o$/kJ mol^{-1}
L1	0.1	7.5	-52.2	-9.6	-42.6
L2	0.2	6.9	-43.5	-4.1	-39.4
	*N*2	log K_a	$\Delta_r H^o$/kJ mol^{-1}	$T\Delta_r S^o$/kJ mol^{-1}	$\Delta_r G^o$/kJ mol^{-1}
L1	0.03	9.7	-38.5	16.8	-55.3
L2	0.1	9.5	-28.2	26.0	-54.2

Table 5. Dimensional values for the poly $(dGdC)_2$ displayed in Figure 5. Letters refer to the respective panels in Figure 5.

	A	**B**	**C**	**D**
Maximal Height (nm)	2.1	4.4	4.0	3.1
Maximal Width (nm)	24	82	76	67